Journal of Applied Polymer Science

# Fabrication and *In Vitro* Investigation of Nanohydroxyapatite, Chitosan, Poly(L-lactic acid) Ternary Biocomposite

**C. Y. Zhang,[1,2] C. L. Zhang,[1] J. F. Wang,[2] C. H. Lu,[2] Z. Zhuang,[1] X. P. Wang,[1] Q. F. Fang[1]**

[1]Key Laboratory of Materials Physics, Institute of Solid State Physics, Chinese Academy of Sciences, Hefei 230031, People's Republic of China

[2]School of Pharmacy, Anhui Traditional Chinese Medical College, Hefei 230038, People's Republic of China

Correspondence to: Q. F. Fang (E-mail: qffang@issp.ac.cn)

**ABSTRACT:** The nanohydroxyapatite/chitosan/poly(L-lactic acid) (HA/CS/PLLA) ternary biocomposites were prepared by blending the hydroxyapatite/chitosan (HA/CS) nanocomposites with poly(L-lactic acid) (PLLA) solution. Surface modification by grafting D-, L-lactic acid onto the HA/CS nanocomposites was designed to improve the bonding with PLLA. The FTIR and $^{13}$C-NMR spectrum confirmed that the oligo(lactic acid) was successfully grafted onto the HA/CS nanocomposites, and the time-dependent phase monitoring showed that the grafted copolymers were stable. The TEM morphology of the HA/CS/PLLA ternary nanocomposites showed that nano-HA fibers were distributed homogeneously, compacted closely and wrapped tightly by the CS and PLLA matrix. The ternary biocomposites with the HA content of 60 and 67 wt % exhibited high compressive strength of about 160 MPa and suitable hydrophilicity. The *in vitro* tests exhibited that the ternary biocomposites have good biodegradability and bioactivity when immersed in SBF solutions. All the results suggested that the *n*-HA/CS/PLLA ternary biocomposites are appropriate to application as bone substitute in bone tissue engineering. © 2012 Wiley Periodicals, Inc. J. Appl. Polym. Sci. 000: 000–000, 2012

**KEYWORDS:** hydroxyapatite nanocomposite; polylactic acid; graft copolymer; biodegradation; bioactivity; bone tissue engineering; *in situ* hybridization

Received 29 December 2011; accepted 21 March 2012; published online
**DOI: 10.1002/app.37795**

## INTRODUCTION

The development of bio-mimetic materials has long been a major goal in the field of bone tissue engineering. Natural bone is a kind of typical organic–inorganic nanocomposite material, which consists of collagen and minerals (apatites) and has an excellent balance between strength and toughness superior to either of its individual components.[1] Therefore, the most promising artificial biomaterials as bone substitutes should be organic–inorganic nanocomposites in which inorganic nanocrystallites disperse in synthetic or natural polymer matrices.[2–4]

Owing to the chemical and biological similarity to the mineral phase of native bone, good biocompatibility, osteoconductivity, and bone-bonding properties,[5,6] hydroxyapatite (HA, $Ca_{10}(PO_4)_6(OH)_2$) was widely considered as guided bone regeneration and bone substitutes[7–9] and preferentially considered as the inorganic parts of the artificial biomaterials. Poly(L-lactic acid) (PLLA), one of the most used synthetic polymer, has attracted wide attention for its biodegradability, biocompatibility, and thermal plasticity. Therefore, composites with incorporation of nano-HA into PLLA matrix would possess good osteoconductivity, osteoinductivity, and mechanical properties at the same time. In addition, the alkalinity of HA can alleviate the particular acidity of PLLA products.

For HA/polymer composites, fine dispersion of HA in the polymer matrix is a critical factor to the properties of the composites. However, the weak interface adhesion of HA with organic phase causes aggregation of HA particles in the PLLA matrix. To achieve uniform HA/PLLA nanocomposite, many approaches were used, including mechanical mixing,[10,11] ultrasound,[12] surface modification,[13,14] *in situ* precipitation,[15,16] etc. It was found that higher HA content resulted in more aggregation and fragile fracture of the HA/PLLA composites.[11–17]

Chitosan (CS), a natural biodegradable polymer, is an *N*-deacetylation product of chitin consisting of glucosamine and *N*-acetylglucosamine units linked through $\beta$-D-(1-4)-glycosidic bonds.[18] Owing to the unique properties such as biodegradability by enzymes in human body, nontoxicity of the degradation product, antibacterial effect, and biocompatibility, CS-based

biomedical materials have attracted much attention.[19–21] It was reported that HA/CS composites show good biocompatibility, bonding ability with surrounding host tissues inherent from HA, tissue regenerative efficacy, and osteoconductivity.[22–25]

CS is a rare natural alkaline polysaccharide, which is soluble or insoluble depending on the pH value of environments.[26] HA is the most basic calcium orthophosphate, which is insoluble in neutral and basic medium.[27] Therefore by manipulating pH value, various methods were used to fabricate HA/CS composites, such as mechanical mixing of HA powders in CS solution,[28,29] coprecipitation,[24,30,31] and *in situ* hybridization.[20,25,32,33] In HA/CS composites, the HA content can reach as high as 90 wt % and the corresponding compressive strength can be obviously enhanced. For example, Zhang et al.[24] has reported that the compressive strength of HA/CS composites can reach about 120 MPa with the HA content of 70 wt %. In one of our previous research,[25] the maximum compressive strength of fibrous HA/CS nanocomposites reached 170 MPa owing to the HA fibers reinforcement in the 50–70 wt % HA/CS composites. However, high brittleness, swelling rate, crystallinity, and water absorption have limited the application of the HA/CS composites in wet physiological environment.

To overcome the shortage of the binary composite of HA/PLLA and HA/CS by combining the advantages of each component, nano-HA/CS/PLLA ternary bio-composites were fabricated in this research. The microstructure, mechanical properties, wetting angle, and the *in vitro* behaviors in simulated body fluid (SBF) of the nano-HA/CS/PLLA ternary bio-composites were investigated.

## MATERIALS AND METHODS

### Materials

Biomedical grade CS (viscosity-average molecular weight $4.5 \times 10^5$) was supplied by Bomei Bioengineering, China with 95% degree of the deacetylation. Poly-L-lactide (PLLA) ($M_w$ : 200,000) is from Shengzhen BrightChina Industrial, China. Calcium hydroxide, acetic acid (glacial), D-, L-Lactic acid (LA), and 85% orthophosphoric acid solution were purchased from Sinopharm Chemical Reagent, China.

### Preparation of HA/CS/PLLA Ternary Nanocomposite

The ternary HA/CS/PLLA bio-composites were fabricated by three steps. Firstly, the HA/CS nanocomposites with high content of HA were obtained by *in situ* hybridization. Then the obtained HA/CS particles were grafted with D-, L-Lactic acid. At last the grafted HA/CS nanocomposites (HA/CS-*g*-LA) were further blended with PLLA matrix.

The HA/CS nanocomposites with the HA content of 80 and 90 wt % were prepared, the details of which were descried in one of our previous work.[34] Briefly, solution of phosphoric acid and CS was dropped slowly into calcium hydroxide solution with vigorous stirring. The aged CS—$Ca(OH)_2$—$H_3PO_4$ slurry was poured into a dialysis bag coated with a CS semipermeable membrane and then immersed into a 2 wt % NaOH aqueous solution to *in situ* hybridize the fibrous HA/CS composite powders.

Subsequently, the obtained HA/CS powders was dispersed into a 2 wt % aqueous LA solution, to protonate the amino groups of CS and to form the CS carboxylic acid ammonium salt according to eq. (1). After stirred for 2 h, the mixture was dried at 65°C for 5 h and then put in a vacuum chamber at 85°C for 4 h to promote dehydration of the CS copolymer salts and the linkage of the corresponding amides. The corresponding grafting reaction was assumed as eq. (2). To remove the unreacted lactic acid and lactic acid oligomer (OLA), the sample was extracted with chloroform and methanol successively in a Soxhlet apparatus for 48 h and designated as the HA/CS-*g*-LA.

**Table I.** The Dosage of Reagents for the Preparation of HA/CS/PLLA Ternary Nanocomposites

| HA ratio (wt %) in HA/CS/PLLA ternary nanocomposites | HA/CS(g) | PLLA(g) | LA (g) | LA/CS (wt/wt) |
|---|---|---|---|---|
| 60 | 1 g (90 wt % HA/CS) | 0.5 | 0.1–0.3 | 1–3 |
| 67 | 1 g (80 wt % HA/CS) | 0.2 | 0.2–0.6 | 1–3 |

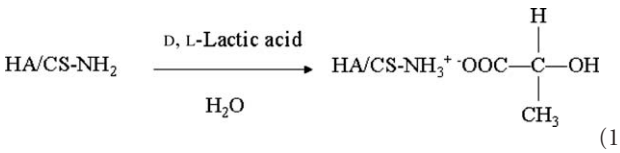


(1)

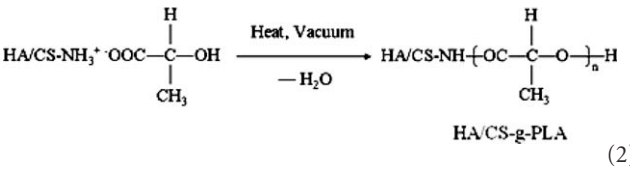


(2)

At last, the obtained HA/CS-*g*-LA powders were added in the solution of the PLA matrix by stirring for 40 min and sonicating for 40 min to form the uniform HA/CS/PLLA ternary nanocomposites. The amounts of the precursors for preparation of the HA/CS/PLLA ternary nanocomposites with HA content of 60 and 67 wt % were listed in Table I.

### Characterization

Compositional determination of the HA/CS-*g*-LA grafted copolymer was characterized by Fourier transform infrared spectroscopy in a Nicolet Nexus spectrometer operating in transmission mode and by the $^{13}$C-NMR spectrum in a Bruker AC-400 NMR spectrometer at 400 MHz in solid state. Time-dependent phase monitoring was carried out to observe the dispersion stability of the HA/CS-*g*-LA powders in the PLLA solution. Transmission electron microscopy (TEM, JEOL-2010) was exploited to detect the microstructure of the microtome layers (Ultracute 970114, Cambridge) of the HA/CS/PLLA ternary nanocomposites.

The compressive strength of the HA/CS/PLLA ternary nanocomposites was evaluated with a CMT4204 mechanical tester (SANS, China). The specimens were cylinders of about 10 mm in diameter and about 20 mm in length prepared by hot pressing at 115°C for 15 min under a pressure of 200 MPa. The crosshead speed

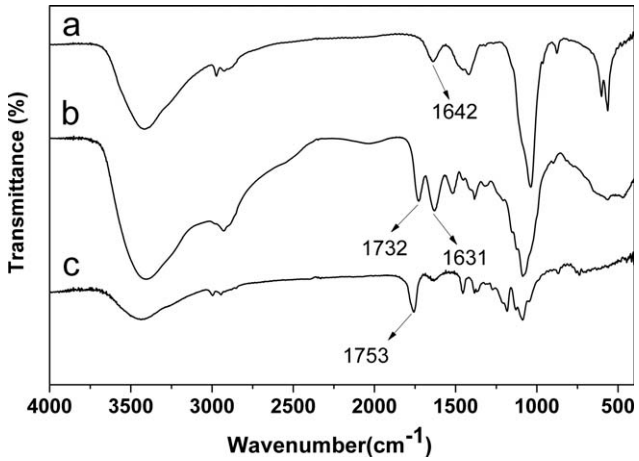


**Figure 1.** (a) FTIR spectra of HA/CS, (b) HA/CS-*g*-LA copolymers (LA/CS = 2 : 1 chloroform- and methanol-extracted), and (c) PLLA.

was set at 1 mm/min, and the load was applied until the samples compressed to 30% of its original length. The compressive strength was determined as the maximum point of the stress–strain curve. Five specimens at one composition were tested and the data was averaged.

Wetting angles were measured on the unpolished basal surface of the specimens of the HA/CS/PLLA ternary nanocomposites with a 5 $\mu$L water droplet (Kruss, Germany). The wetting angle was fitted with the Young-Laplace's equation. Measurements were made in triplicate on each specimen and the data was averaged.

The *in vitro* tests were performed in SBF to investigate the biodegradability and bioactivity of HA/CS/PLLA ternary nanocomposites. The hot-pressed specimens were immersed in SBF[35] at 37°C for 2, 4, and 6 weeks. The microstructures and crystal phases of these specimens after soaking were analyzed by scanning electron microscope (SEM) with Energy dispersive spectroscopy (EDS, Oxford INCA). Calcium concentrations in the SBF solutions were measured as a function of soaking time with inductively coupled plasma atomic emission spectroscope (ICP). The pH value of the lixiviums was measured by the Automatic Potentiometric Titrator (JENCO, America).

## RESULTS AND DISCUSSION

### FTIR Analysis of HA/CS-*g*-LA Grafted Copolymer

Figure 1 showed the IR spectra of the HA/CS-*g*-LA copolymer after extracting with chloroform and methanol [Figure 1(b)], where the results of HA/CS [Figure 1(a)] and pure PLLA [Figure 1(c)] were also shown for comparison. In the IR spectrum of the HA/CS [Figure 1(a)] the characteristic peaks of CS and HA appear as analyzed in our previous work.[25] In brief, the peaks at 1092, 1036, 962, 604, and 565 $cm^{-1}$ correspond to different vibration modes of $PO_4^{3-}$ group and 3569 $cm^{-1}$ can be assigned to the stretching vibrations of $OH^-$ group in HA. The characteristic peaks of CS at 2930–2850 $cm^{-1}$ correspond to the —CH backbone stretching vibrations and the bands at 1153, 1084, and 1028 $cm^{-1}$ correspond to the C—O stretching vibrations pertinent to the glucosamine unit. Specifically, the peak around 1642 $cm^{-1}$ can be assigned to the overlapping of the peaks of the amide bands I and II of CS in the HA/CS

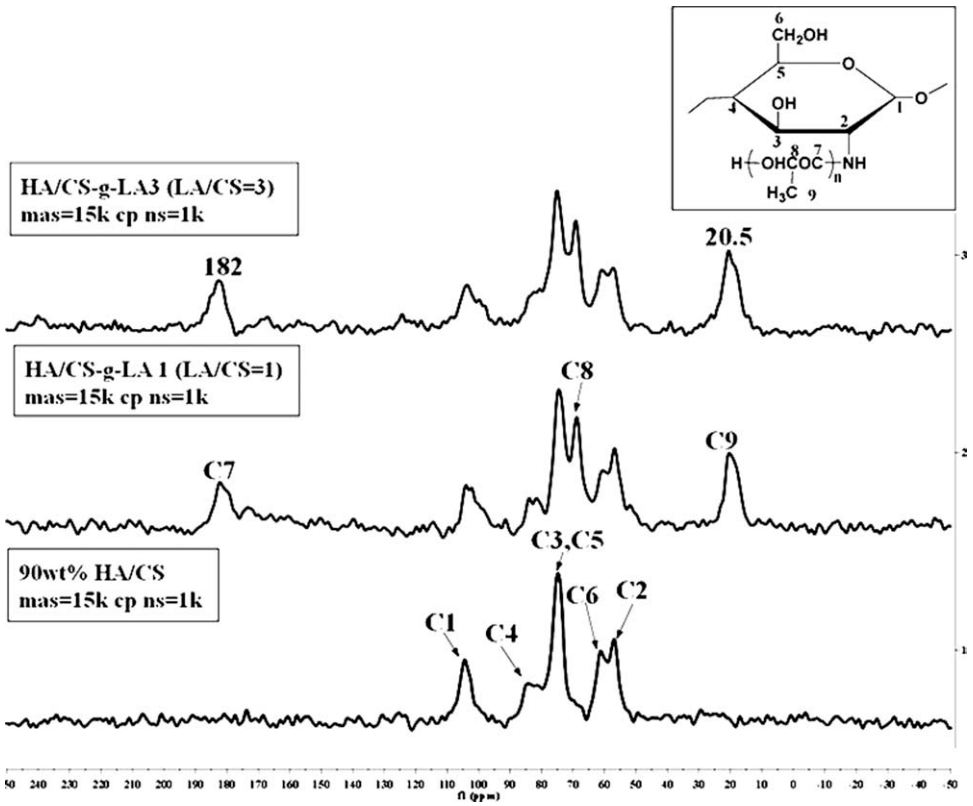


**Figure 2.** $^{13}$C-NMR spectrum of HA/CS and HA/CS-*g*-LA graft copolymer (chloroform- and methanol-extracted).

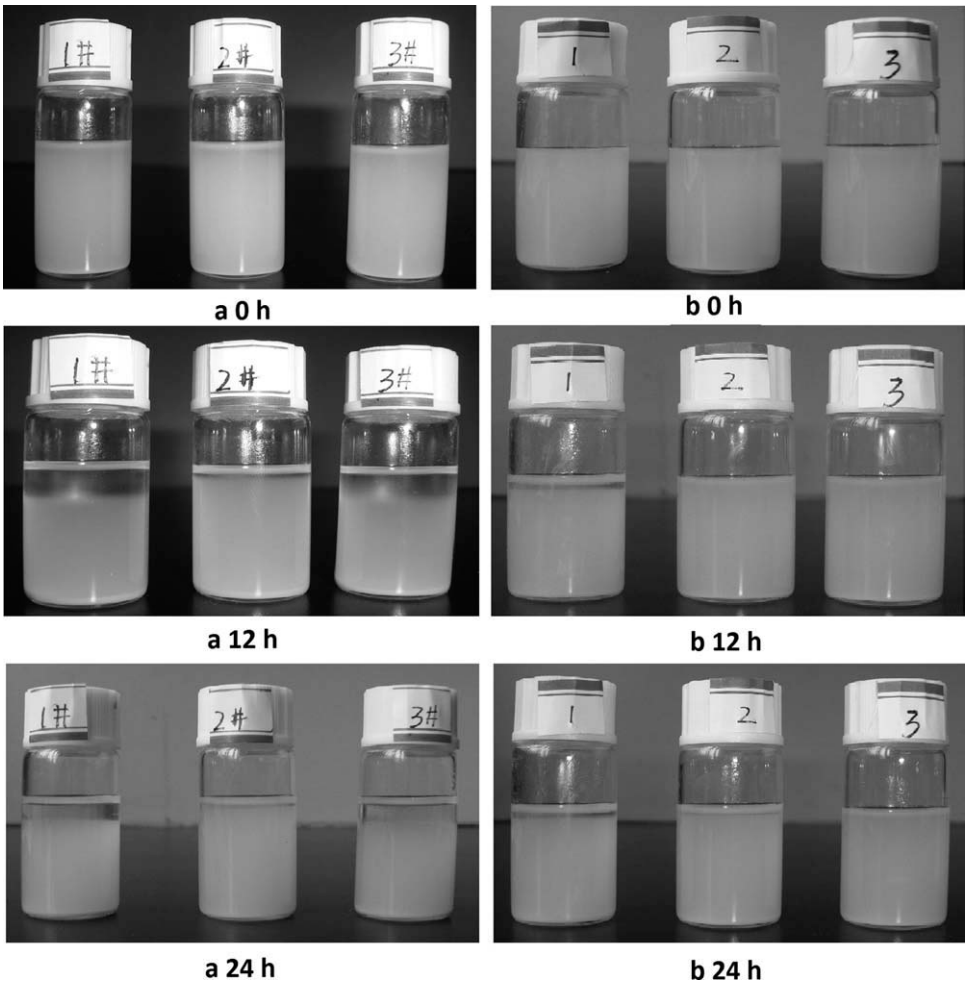


**Figure 3.** Time-dependent phase behavior of the mixture of the HA/CS-*g*-LA graft copolymer in different solvent (a) (1#: tolerant; 2#: dioxane; 3#: dimethylformamide) and with different feed ratio of LA/CS (wt/wt) (1: LA/CS = 1; 2: LA/CS = 2; 3: LA/CS = 3) in dioxane (b).

nanocomposites. In the HA/CS-*g*-LA copolymer after extracting by chloroform and methanol [Figure 1(b)], the sharp peak around 1732 $cm^{-1}$ can be ascribed to the carbonyl absorption of the ester or carboxylic groups of OLA,[36–38] which was shifted about 20 wave numbers in comparison with the carbonyl absorption peak at 1753 $cm^{-1}$ in the pure PLLA [Figure 1(c)]. It can be seen that the peak at 1642 $cm^{-1}$ in the HA/CS [Figure 1(a)] attributed to the amide groups shifted to 1631 $cm^{-1}$ in the HA/CS-*g*-LA copolymer [Figure 1(b)]. The above evidences indicate that the amidation reaction indeed occurred between CS and LA or OLA and hydrogen bonds may be formed between the ester groups of OLA and amino or hydroxyl groups of CS.

### $^{13}$C-NMR Analysis of HA/CS-*g*-LA Graft Copolymer

The $^{13}$C-NMR spectrum of the HA/CS and HA/CS-*g*-LA grafted copolymers of LA/CS = 1 : 1 and 3 : 1 were compared in Figure 2. The $^{13}$C-NMR spectrum of the HA/CS powders showed the characteristic saccharine structure of the CS with the signals at 103 (C1), 83 (C4), 74 (C3 and C5), 61 (C6), and 57 ppm (C2) along the increase of the magnetic field.[37] The overlapping of the C3 and C5 was mainly caused by the glycosidation shift effect of the C4. In the $^{13}$C-NMR spectrum of the chloroform- and methanol-extracted HA/CS-*g*-LA grafted copolymers, there were three new peaks appeared except for the signals of CS. The peak at 182 ppm was attributed to the carbonyl carbon (C7) and the peaks at 20.5 and 70 ppm were assigned to the methyl (C9) and methane (C8) carbons of the OLA side chain as shown in Figure 2. These evidences obviously confirmed that the OLA side chain was grafted onto the CS main chain in the HA/CS. At the same time the above new signals of the OLA side chain became stronger with the increasing of the feed ratio of LA/CS, indicating the increase of the amount of grafted OLA.

### Time-Dependent Phase Behavior and Microscopy Analysis

After the HA/CS was grafted with OLA, the obtained HA/CS-*g*-LA powders would be more stable and uniform in the PLLA solution by tethering to the molecular chains of PLLA matrix. The time-dependent phase monitoring was used to observe the dispersion stability of the HA/CS-*g*-LA powders in the PLLA solution within a certain period of time.

The HA/CS-*g*-LA powders were added separately in tolerant, dimethylformamide, and dioxane solution of the PLLA by stirring and sonicating for 40 min, and the phase behavior of each

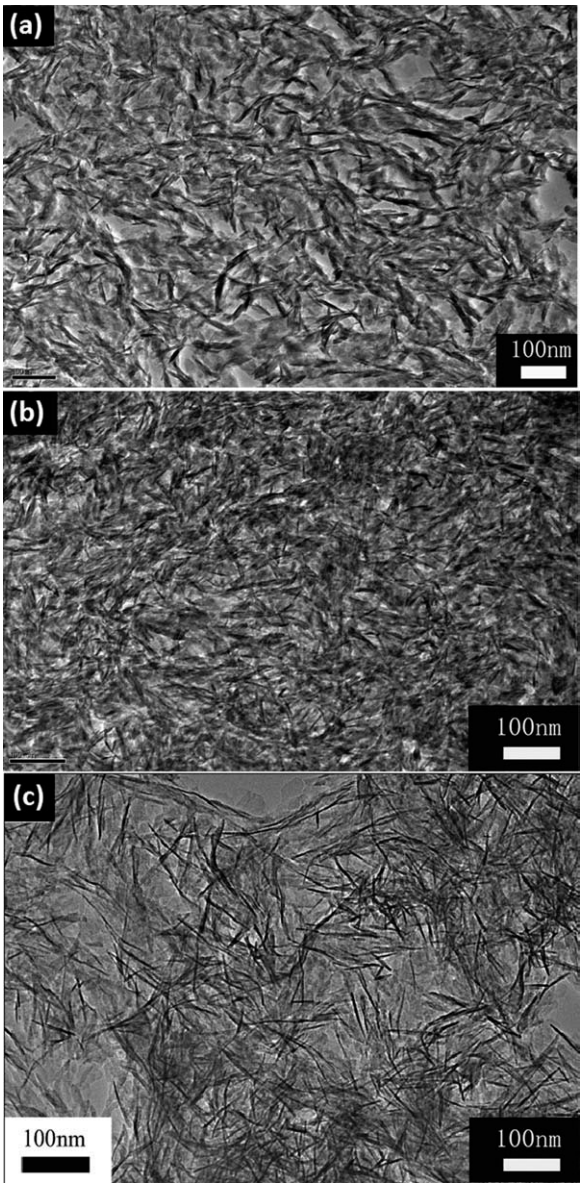


**Figure 4.** TEM microscopes of the HA/CS/PLLA ternary nanocomposites with the HA content of (a) 60 wt % and (b) 67 wt%, and (c) the fibrous HA/CS nanocomposites.

mixture was monitored at room temperature after equilibrating for 24 h. The colloidal stability of the HA/CS-*g*-LA powders in different mixtures was shown in Figure 3(a). It can be seen that dioxane is more suitable for the HA/CS-*g*-LA powders mixed with the PLLA matrix. As for the dosage of LA for grafting, LA/CS (wt/wt) = 1, 2, and 3 were chosen, and the corresponding phase behavior were shown in Figure 3(b). The result indicated that LA/CS = 2 was sufficient to maintain the colloidal stability within 24 h.

On the basis of the above phase behavior, it can be assumed that the HA/CS-*g*-LA powders in dioxane solution of the PLLA could produce HA/CS/PLLA ternary nanocomposites with uniform dispersion and homogeneous properties. Figure 4 presented the TEM microscopes of the HA/CS/PLLA ternary nanocomposites with the HA content of 60 and 67 wt %. As can be seen in Figure 4(a,b), there were evenly spatial distribution of fibrous HA crystals throughout the CS/PLLA matrix with the high HA content, owing to the stable suspension of HA/CS-*g*-LA powders in the PLLA solution. Compared with the HA/CS nanocomposite [Figure 4(c)], the HA fibers in the HA/CS/PLLA ternary nanocomposites were compacted closely and wrapped tightly. It is mainly due to the bonding and adhesion of the PLLA matrix to the HA/CS-*g*-LA powders, which would effectively prevent the HA flowing from the HA/CS/PLLA ternary nanocomposites under the liquid impact *in vitro* and *in vivo*.

### Mechanical Properties

For HA/polymer nanocomposites, it is critical to obtain homogeneous structure as well as uniformly distributed HA at nano-level.[39] In the HA/CS/PLLA ternary nanocomposites, uniformly dispersed nano-HA crystals with good links to the matrix would improve further the final mechanical properties. Figure 5 illustrated the typical compressive stress–strain plot of the HA/CS/PLLA ternary nanocomposites. It can be seen from Figure 5(a) that the compressive strength can reach 160 MPa at the HA content of 60 and 67 wt %. When compared with the stress–strain curves of the HA/CS nanocomposites in Figure 5(b), the

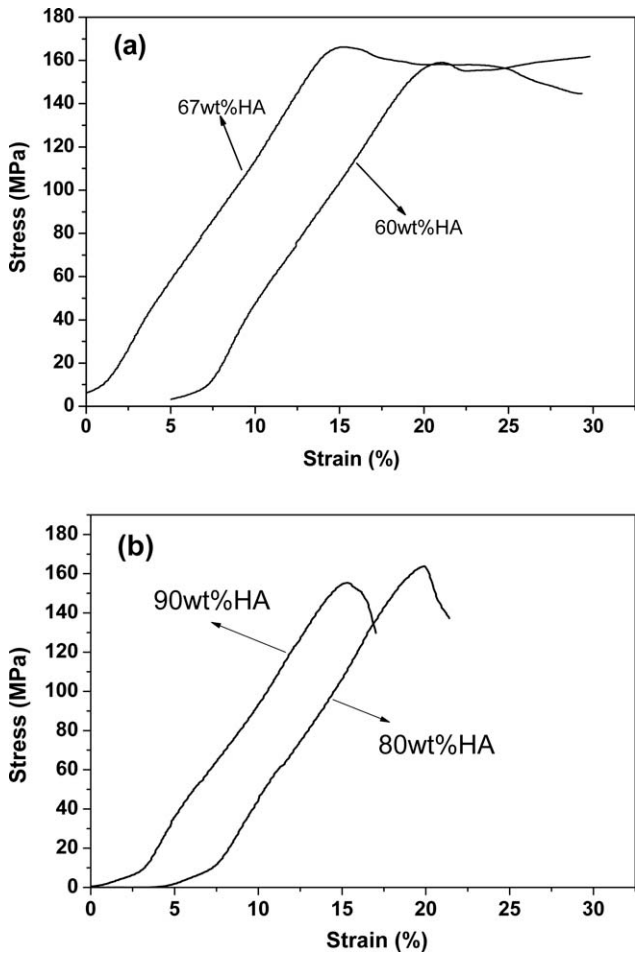


**Figure 5.** The stress–strain curves in compression of the HA/CS/PLLA (a) ternary nanocomposites and (b) fibrous HA/CS nanocomposites.

Applied Polymer SCIENCE

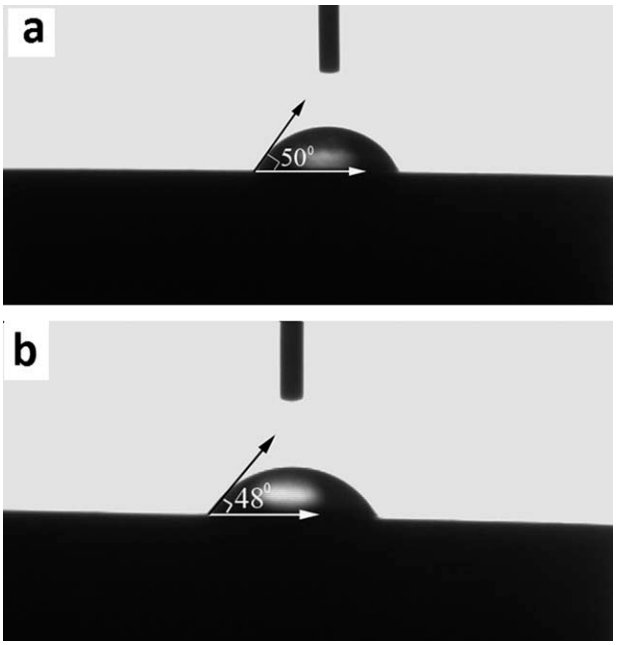


**Figure 6.** The wetting angles of the HA/CS/PLLA ternary nanocomposites with the HA content of (a) 60 wt % and (b) 67 wt %.

HA/CS/PLLA ternary nanocomposites exhibit better toughness from the yield mode in the compressive test. Combined the high compressive strength of the HA/CS nanocomposites and the ductile performance of the PLLA, the HA/CS/PLLA ternary nanocomposites possess ideal mechanical properties for bone tissue engineering and loaded-bearing bone defects repairing.

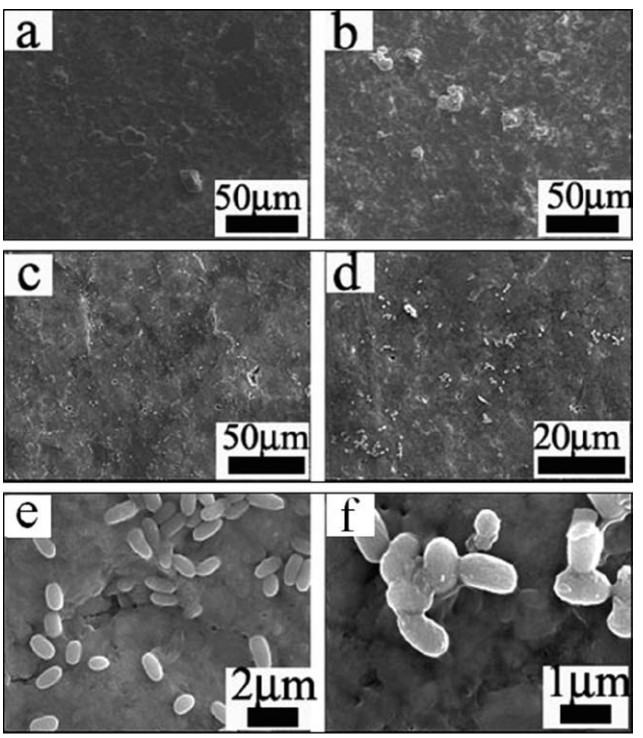


**Figure 7.** SEM images of the nano-HA/CS/PLLA ternary biocomposites after soaked in the SBF solution for (a) 0, (b) 2, (c) 4, and (d–f) 6 weeks.

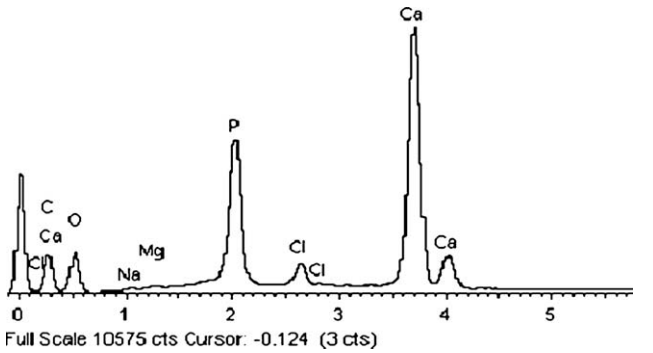


**Figure 8.** EDS spectra of the granules depositing on the HA/CS/PLLA ternary nanocomposites after soaked in SBF solution for 6 weeks.

### Wetting Angles

The wetting angles of the HA/CS/PLLA ternary nanocomposites were shown in Figure 6. The contact angles of the ternary nanocomposites with HA content of 60 and 67 wt % are 50° and 48°, respectively, indicating that the HA/CS/PLLA ternary nanocomposites were hydrophilic. Because HA and CS are more hydrophilic than PLLA, the presence of HA and CS decreases the wetting angle and thus improves wettability in the HA/CS/PLLA ternary nanocomposites. According to Ref. 40, such hydrophilic contact angles are suitable for cell adhesion and growth on the surface, ensuring the biocompatibility performance *in vivo*.

### *In Vitro* Assay in SBF

The specimens of HA/CS/PLLA ternary nanocomposites were soaked in SBF for different periods of time to investigate its biodegradation and bioactivity *in vitro*. Figure 7 showed the microstructures of the specimens after soaking in SBF solutions at 37°C for 2, 4, and 6 weeks. Compared with the specimen before soaking [Figure 7(a)], the surfaces of the soaked specimens become more rough. After 2 weeks soaking in SBF [Figure 7(b,c)], a lot of tiny particles were deposited and some pores were formed on the surface. After 6 weeks soaking [Figure 7(d)], there were more porous defects and more granules deposited on the surface of the specimens. As revealed in high

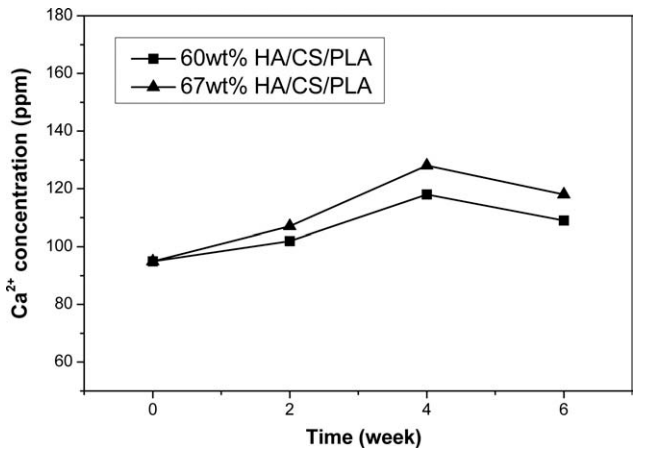


**Figure 9.** $Ca^{2+}$ concentration in SBF as a function of the soaking time of the HA/CS/PLLA ternary nanocomposites.

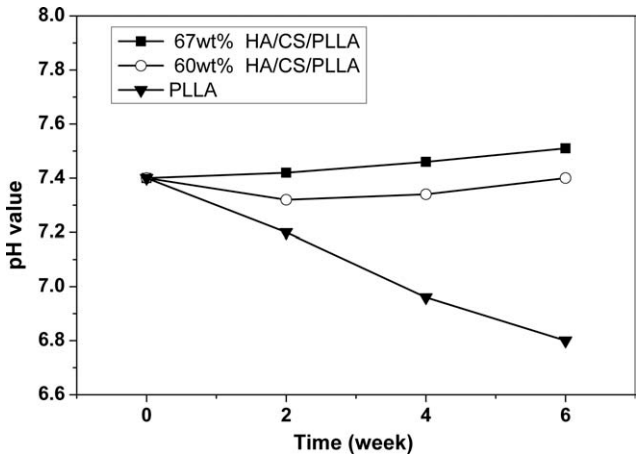


**Figure 10.** The pH value of the lixiviums as a function of the soaking time of the HA/CS/PLLA ternary nanocomposites and PLLA.

magnifications in Figure 7(e,f), these granules are silkworm-like with an average size of about 1 $\mu$m in length and 600 nm in width and attached firmly to the surface of the specimens. In fact, these granules seemingly grow from the surface of the specimens.

From the EDS spectra shown in Figure 8, it can be seen that except for elements Cl, Na, and Mg that come from the SBF, the main elements in these silkworm-like granules are Ca, P, and O, and the Ca/P molar ratio was about 1.73, which is close to the stoichiometric composition of HA (1.67). That is to say, the granules deposited on the surface of the HA/CS/PLLA ternary nanocomposites are mainly consisted of bone-like apatite crystals. These results indicated that the HA/CS/PLLA ternary nanocomposites exhibited a proper response to the simulated body environment, making the composite promising for biomedical applications *in vivo*.

$Ca^{2+}$ concentration in the SBF as a function of soaking time was shown in Figure 9. It can be seen that $Ca^{2+}$ concentration increased within the previous 4 weeks soaking and then decreased slowly. It has been generally accepted that the formation of bone-like apatite crystals in simulated body environment is the balance of dissolution-deposition process.[41–43] For the HA/CS/PLLA ternary nanocomposites, the increase of the $Ca^{2+}$ concentration before 4 weeks soaking was possibly because of the dissolution of HA in the soaking specimen exceeding the apatite deposition. The higher $Ca^{2+}$ concentration would promote the deposition process and more silkworm-like granules deposited and grown, resulting in the decrease of $Ca^{2+}$ concentration in SBF after long soaking. Calcium release and deposition is an important symbol of biological activity, especially in the tissue binding capacity for biomaterials, and indicates the competition between the dissolution-deposition processes of HA on the surface of the HA/CS/PLLA ternary nanocomposites in SBF.

Figure 10 showed the variation of pH value of the lixiviums during the *in vitro* assay with the soaking time. For the pure PLLA the pH value of the lixivium decreases greatly with the soaking time owing to the acid degradation products of PLLA. For the HA/CS/PLLA ternary nanocomposites with the HA content of 60 and 67 wt %, the pH values are almost constant with small fluctuation between 7.34 and 7.51 during the whole 6 weeks soaking. Such pH value would favor the formation of apatite and release of the $Ca^{2+}$ *in vitro*.[44] The stable pH value was resulted mainly from the fact that the alkaline degradation products of the HA and CS would neutralize the degradation products of the PLLA. Therefore, the HA/CS/PLLA ternary nanocomposites would not induce the inflammatory reaction as implanting biomaterials for bone tissue engineering.

## CONCLUSION

In this study, the HA/CS/PLLA ternary nanocomposites were fabricated by grafting HA/CS nanocomposites with LA and further blending with the PLLA matrix. FTIR and $^{13}$C-NMR spectrum confirmed the OLA was successfully grafted onto the CS in the HA/CS and the obtained HA/CS-*g*-LA copolymer were stable and uniformly distributed in the PLLA solution. The nano-HA/CS/PLLA ternary bio-composites showed high compressive strength of about 160 MPa and better toughness with the HA content of 60 and 67 wt %, and their wetting angels were suitable for cell adhesion and growth. The *in vitro* test of the HA/CS/PLLA nanocomposites showed that the porous defects appeared and the bone-like apatite deposited and grew up on the surface with small variation of pH value in the SBF solution. All the results indicated that the nano-HA/CS/PLLA ternary bio-composites possess better mechanical properties, good biodegradability, and bioactivity, which have promising application as bone substitute in bone tissue engineering.

## ACKNOWLEDGMENTS

The authors appreciate Dr. Chun Li at Nanchang Hangkong University for her help in the compression experiments. This work was supported by Natural Science Foundation (10040606Q36) and Provincial Natural Science Foundation for Colleges and Universities (KJ2012ZD09) of Anhui Province.

## REFERENCES

1. Kikuchi, M.; Itoh, S.; Ichinose, S.; Shinomiya, K.; Tanaka, J. *Biomaterials* **2001,** *22*, 1705.
2. Rezwan, K.; Chen, Q. Z.; Blaker, J. J.; Boccaccini, A. R. *Biomaterials* **2006,** *27*, 3413.
3. Wei, G.; Ma, P. X. *Biomaterials* **2004,** *25*, 4749.
4. Murugan, R.; Ramakrishna, S. *Appl. Phys. Lett.* **2006,** *88*, 193124.
5. Hench, L. L.; Wilson, J. *Science* **1984,** *226*, 630.
6. Shackelford, J. F. *Mater. Sci. Forum.* **1999,** *293*, 99.
7. Ducheyne, P. *J. Biomed. Mater. Res. B* **1987,** *21*, 219.
8. Kitsugi, T.; Yamamuro, T.; Nakamura, T.; Kotani, S.; Kokubo, T.; Takeuchi, H. *Biomaterials* **1993,** *14*, 216.
9. Best, S.; Bonfield, W. *J. Mater. Sci: Mater. Med.* **1994,** *5*, 516.
10. Ignjatovie, N.; Uskokovic, D. *Appl. Surf. Sci.* **2004,** *238*, 314.
11. Nikcevic, I.; Maravic, D.; Ignjatovic, N.; Mitric, M.; Makovec, D.; Uskokovic, D. *Mater. Trans.* **2006,** *47*, 2980.

12. Fang, Y.; Agrawal, D. K.; Roy, D. M.; Roy, R.; Brown, P. W. *J. Mater. Res.* **1992,** *7*, 2294.
13. Hong, Z. K.; Zhang, P. B.; He, C. L.; Qiu, X. Y.; Liu, A. X.; Chen, L.; Chen, X. S.; Jing, X. B. *Biomaterials* **2005,** *26*, 6296.
14. Liu, Q.; de Wijn, J. R.; van Toledo, M.; Bakker, D.; van Blitterswijk, C. A. *J. Mater. Sci: Mater. Med.* **1998,** *9*, 23.
15. Zhang, C. Y.; Lu, H.; Zhuang, Z.; Wang, X. P.; Fang, Q. F. *J. Mater. Sci: Mater. Med.* **2010,** *21*, 3077.
16. Xiao, Y. M.; Zhao, H. C.; Fan, H. S.; Wang, X. L.; Guo, L. K.; Li, X. D.; Zhang, X. D. *Mater. Sci. Forum.* **2005,** *475–479*, 2383.
17. Tian, T.; Jiang, D. L.; Zhang, J. X.; Lin, Q. L. *Mater. Sci. Eng. C* **2008,** *28*, 51.
18. Mi, F. L.; Tan, Y. C.; Liang, H. F.; Sung, H. W. *Biomaterials* **2002,** *23*, 181.
19. Wang, L. H.; Khor, E.; Wee, A.; Lim, L. Y. *J. Biomed. Mater. Res. A* **2002,** *63*, 610.
20. Hu, Q. L.; Li, B. Q.; Wang, M.; Shen, J. C. *Biomaterials* **2004,** *25*, 779.
21. Kumar, R.; Prakash, K. H.; Cheang, P.; Gower, L.; Khor, K. A. *J. R. Soc. Interface.* **2008,** *5*, 427.
22. Wang, X. H.; Ma, J. B.; Wang, Y. N.; He, B. L. *Biomaterials* **2002,** *23*, 4167.
23. Kong, L. J.; Gao, Y.; Cao, W. L.; Gong, Y. D.; Zhao, N. M.; Zhang, X. F. *J. Biomed. Mater. Res. A* **2005,** *75*, 275.
24. Zhang, L.; Li, Y. B.; Yang, A. P.; Peng, X. L.; Wang, X. J.; Zhang, X. *J. Mater. Sci.: Mater. Med.* **2005,** *16*, 213.
25. Zhang, C. Y.; Chen, J.; Zhuang, Z.; Zhang, T.; Wang, X. P.; Fang, Q. F. *J. Appl. Polym. Sci.* **2012,** DOI: 10.1002/app.35103.
26. Domard, A. *Int. J. Biol. Macromol.* **1987,** *9*, 98.
27. Viala, S.; Freche, M.; Lacout, J. L. *Ann. Chim.-Sci. Mater.* **1998,** *23*, 69.
28. Yin. Y. J.; Zhao, F.; Song, X. F.; Yao, K. D.; Lu, W. W.; Leong, J. C. *J. Appl. Polym. Sci.* **2000,** *77*, 2929.
29. Thein-Han, W. W.; Misra, R. D. *Acta. Biomater.* **2009,** *5*, 1182.
30. Yamaguchi, I.; Tokuchi, K.; Fukuzaki, H.; Koyama, Y.; Takakuda, K.; Monma, H.; Tanaka, T. *J. Biomed. Mater. Res.* **2001,** *55*, 20.
31. Sreedhar, B.; Aparna, Y.; Sairam, M.; Hebalkar, N. *J. Appl. Polym. Sci.* **2007,** *105*, 928.
32. Kong, L. J.; Gao, Y.; Cao, W. L.; Gong, Y. D.; Zhao, N. M.; Zhang, X. F. *J. Biomed. Mater. Res. A.* **2005,** *75*, 275.
33. Zhang, Y. Z.; Venugopal, J. R.; El-Turki, A.; Ramakrishna, S.; Su, B.; Lim, C. T. *Biomaterials* **2008,** *29*, 4314.
34. Zhang, C. Y.; Peng, D. Y.; Lu, C. H.; Zhuang, Z.; Wang, X. P.; Fang, Q. F. *Adv. Mater. Res.* **2012,** *457–458*, 365.
35. Oyane, A.; Nakanishi, K.; Kim, H. M.; Miyaji, F.; Kokubo, T.; Soga, N.; Nakamura, T. *Biomaterials* **1999,** *20*, 79.
36. Wu, Y.; Zheng, Y. L.; Yang, W. L.; Wang, C. C.; Hu, J. H.; Fu, S. K. *Carbohyd. Polym.* **2005,** *59*, 165.
37. Yao, F. L.; Chen, W.; Wang, H.; Liu, H. F.; Yao, K. D.; Sun, P. C.; Lin, H. *Polymer* **2003,** *44*, 6435.
38. Qu, X.; Wirsen, A.; Albertsson, A.-C. *Polymer* **2000,** *41*, 4589.
39. Lee, H. J.; Kim, S. E.; Choi, H. W.; Kim, C. W.; Kim, K. J.; Lee, S. C. *Eur. Polym. J.* **2007,** *43*, 1602.
40. Gogolewski, S.; Galletti, G. *Life. Support. Systems.* **1983,** *2*, 324.
41. Hench, L. L. *J. Am. Ceram. Soc.* **1991,** *74*, 1487.
42. Hench, L. L.; Polak, J. M. *Science* **2002,** *295*, 1014.
43. de Sena, L. A.; Rocha, N. C. C.; Andrade, M. C.; Soares, G. A. *Surf. Coat. Tech.* **2003,** *166*, 254.
44. Kokubo, T. *An. Quim. Int. Ed.* **1997,** *93*, 49.